

# Rapid and reversible changes in dendrite morphology and synaptic efficacy following NMDA receptor activation: implication for a cellular defense against excitotoxicity

Yuji Ikegaya<sup>1,\*‡</sup>, Jeong-Ah Kim<sup>1,\*</sup>, Minami Baba<sup>2</sup>, Takeshi Iwatsubo<sup>2</sup>, Nobuyoshi Nishiyama<sup>1</sup> and Norio Matsuki<sup>1</sup>

<sup>1</sup>Laboratory of Chemical Pharmacology and <sup>2</sup>Department of Neuropathology and Neuroscience, Graduate School of Pharmaceutical Sciences, The University of Tokyo, Tokyo 113-0033, Japan

\*These authors contributed equally to this work

‡Author for correspondence (e-mail: ikegaya@tk.airnet.ne.jp)

Accepted 3 August 2001

Journal of Cell Science 114, 4083-4093 (2001) © The Company of Biologists Ltd

## SUMMARY

Postsynaptic neuronal dendrites undergo functional and morphological changes in response to pathologically excessive synaptic activation. Although rapid formation of segmental focal swelling (varicosity) is the most prominent hallmark in such excitotoxic injury, little is known about the pathophysiological function of these structural alterations. We used cultured rat hippocampal slices to evaluate the relationship between the formation of varicosities and subsequent neuronal death. Substantial numbers of segmental dendritic varicosities were observed all over the hippocampus within 5 minutes of exposure to 30  $\mu$ M NMDA, although neuronal death was detected only in the CA1 region 24 hours after NMDA exposure. Sublethal NMDA concentrations (1-10  $\mu$ M) induced reversible focal swelling in all hippocampal subregions. NMDA-induced neuronal death was prevented either by NMDA receptor antagonists or by the use of  $\text{Ca}^{2+}$ -free medium, whereas varicosity formation was virtually independent of  $\text{Ca}^{2+}$  influx. Rather, the  $\text{Ca}^{2+}$ -free

conditions per se produced dendritic focal swelling. Also, NMDA-induced varicosity formation was dependent on extracellular  $\text{Na}^+$  concentration. Thus, we believe that varicosity formation is not causally related to neuronal injury and that the two phenomena are separable and involve distinct mechanisms. Interestingly, dendrite swelling was accompanied by AMPA receptor internalization and a rapid, long-lasting depression in synaptic transmission. Moreover, low  $\text{Na}^+$  conditions or treatment with ethacrynic acid or proteinase inhibitors, which effectively prevent varicosity formation, aggravated NMDA-induced excitotoxicity, and eliminated the regional specificity of the toxicity. Therefore, the pathological changes in dendrite morphology and function may be associated with an early, self-protective response against excitotoxicity.

Key words: *N*-methyl-D-aspartate, Hippocampus, Dendrite, Spine, Excitotoxicity, Varicosity, Swelling, Sodium

## INTRODUCTION

Neuronal cell loss is a common symptom of numerous neurological disorders including Alzheimer's disease, Parkinson's disease, prion disease and Down's syndrome (Coyle and Puttfarcken, 1993; Kakizuka, 1998; Nagy, 1999). Most attention has been focused on 'excitotoxicity' as a mechanism of neuronal death in acute and chronic neurologic diseases (Choi and Rothman, 1990; Shaw, 1993). Cerebral ischemia, head and spinal cord injury and prolonged seizure activity are associated with the excessive release of glutamate into the extracellular space and subsequent neurotoxicity (Bittigau and Ikonomidou, 1997). Accumulating evidence also suggests that impairment of intracellular energy metabolism increases neuronal vulnerability to glutamate, which can damage neurons even at physiologic concentrations. This type of excitotoxicity is likely to be involved in chronic neurodegenerative diseases such as mitochondrial

encephalomyopathies (Shoubridge, 1998), Huntington's disease (Young, 1997) and motor neuron diseases (Jackson and Bryan, 1998). Elucidating mechanisms underlying excitotoxicity may therefore offer a therapeutic approach to treating these disorders.

The dendrite is a major site of excitatory synaptic input between neurons in the central nervous system. Long-term changes in synaptic interaction are assumed to involve alterations in dendrite morphology. Indeed, recent studies have reported structural changes associated with synaptic plasticity (Buchs and Muller, 1996; Maletic-Savatic et al., 1999). At the same time, under pathological conditions of excessive synaptic activation, the dendrite may be selectively vulnerable to neuronal injury because the receptors for excitatory amino acids that mediate excitotoxicity are localized predominantly in the dendrite (Racca et al., 2000). Indeed, a number of pathomorphological studies have correlated diverse forms of dendritic injury with pathological degeneration. A common

feature of dendritic injury is the formation of focal or varicose swelling (varicosity) along the length of the dendritic arbor (Ramón y Cajal, 1909; Olney, 1971; Ikonomidou et al., 1989). This pattern of dendrite swelling has been observed in experimental injury models both in vivo (Hori and Carpenter, 1994; Matesic and Lin, 1994) and in vitro (Bindokas and Miller, 1995; Al-Noori and Swann, 2000). However, the cellular mechanisms underlying the pathological changes in dendrite structure remain to be determined, and little is known about the relationship between these structural changes and neuronal survival.

Using cultured mouse cortical neurons, Park et al. (Park et al., 1996) indicated that NMDA receptor-dependent dendritic varicosity formation occurs even after brief sublethal excitotoxic exposure, and thereafter recovers spontaneously. This varicosity formation was not attenuated in  $\text{Ca}^{2+}$ -free solution (Hasbani et al., 1998), although  $\text{Ca}^{2+}$  is generally believed to be essential for triggering neuronal death (Choi, 1992). On the basis of these observations, we hypothesized that structural changes in dendrites under pathological conditions are not causally associated with neuronal injury. Thus, we have focused the present study on the relationship between varicosity formation and subsequent neuronal death, which have previously been considered inextricably linked. Here we describe a new aspect of NMDA receptor-mediated focal swelling.

## MATERIALS AND METHODS

### Materials

NMDA, MK-801, kainate, veratridine, colchicine, amiloride, furosemide and ethacrynic acid were purchased from Sigma (St Louis, MO). AMPA was obtained from Research Biochemicals (Natick, MA). Latrunculin A, cytochalasin D, tetrodotoxin,  $\text{HgCl}_2$  and protease inhibitor mixture were obtained from Wako Chemicals (Osaka, Japan). Nocodazole was obtained from Calbiochem (La Jolla, CA). Veratridine, amiloride, latrunculin A, cytochalasin D and nocodazole were dissolved in DMSO. Furosemide was dissolved in methanol. The remaining materials listed were dissolved in distilled water. Immediately before use, stock solutions were diluted with culture medium so that the final concentration of DMSO or methanol was less than 0.1%. The presence of 0.1% DMSO or 0.1% methanol had no apparent effect on varicosity formation (data not shown).

### Organotypic cultures of hippocampal slices

Hippocampal slice cultures were prepared from 8-9-day-old Wistar/ST rats (SLC, Shizuoka, Japan), as previously described (Ikegaya, 1999). Animals were deeply anesthetized by hypothermia and their brains were aseptically removed and cut into transverse slices (300  $\mu\text{m}$  thick) in aerated, ice-cold Gey's balanced salt solution supplemented with 25 mM glucose, using a vibratome (DTK-1500; Dosaka, Kyoto, Japan). The hippocampi were dissected out under stereomicroscopic control. Then, selected slices were cultured using membrane interface techniques. Briefly, slices were placed on 30 mm sterile membranes (Millicell-CM, Millipore, Bedford, MA) and transferred into six-well tissue culture trays. Cultures were fed with 1 ml of culture medium consisting of 50% minimal essential medium (Life Technologies, Grand Island, NY), 25% horse serum (Cell Culture Lab, Cleveland, OH) and 25% Hanks' balanced salt solution (HBSS) containing 25 mM glucose, 50 U/ml penicillin G and 100  $\mu\text{g}/\text{ml}$  streptomycin. The cultures were maintained in a humidified incubator at 37°C in 5%  $\text{CO}_2$ . The medium was changed every 3.5 days. Experiments were performed after 12-13 days in vitro.

### Excitotoxin exposure

NMDA, kainate, AMPA and veratridine were added to culture medium at 37°C for 10 minutes. Colchicine, latrunculin A, cytochalasin D and nocodazole were added to culture medium for 12 hours. In some experiments, cultures were transferred to  $\text{Ca}^{2+}$ -free, low  $\text{Na}^+$  or hyperosmotic media 30 minutes before NMDA exposure.  $\text{Ca}^{2+}$ -free solution was prepared by replacing  $\text{CaCl}_2$  in HBSS with 1 mM EDTA (Wako) and 25 mM glucose. Reduced  $\text{Na}^+$  solution was prepared by replacing NaCl in HBSS with 120 mM choline chloride (Wako) and 25 mM glucose (Wako). Hyperosmotic medium was prepared by supplementing HBSS with 200 mM sucrose (Wako). MK-801, tetrodotoxin,  $\text{HgCl}_2$ , amiloride, furosemide and ethacrynic acid were applied 30 minutes prior to NMDA exposure. Protease inhibitor mixture was applied 12 hours prior to NMDA exposure. Recovery experiments were conducted in normal culture medium at 37°C for up to 168 hours.

### Assessment of cell death

Cell death was assessed by propidium iodide (PI) (Molecular Probes, Eugene, OR) fluorescence. PI is a polar compound that only enters cells with damaged membranes and becomes brightly fluorescent red after binding to nucleic acids (Macklis and Madison, 1990). PI was added to culture medium at a final concentration of 5  $\mu\text{g}/\text{ml}$  and the cultures were kept at 37°C for 24 hours. PI fluorescence images were obtained with a BioRad MRC-1000 confocal imaging system (BioRad Microscience Division, Cambridge, MA) equipped with an inverted microscope ECLIPSE TE300 (Nikon, Tokyo, Japan), an argon ion laser and a host computer system. All imaging and processing operations were performed with Laser Sharp Acquisition (Biorad) and Laser Sharp Processing (Biorad), respectively. Pixel intensity of fluorescence (8-bit intensity levels) was measured at three different areas of the slice: the CA1 and CA3 stratum pyramidale and the stratum granulosum of the dentate gyrus (DG). Average intensity ( $F_i$ ) was estimated for each slice by acquiring intensity values in ten different areas (10 $\times$ 400  $\mu\text{m}^2$ ) within each hippocampal subregion. Simultaneously, the background intensity ( $F_0$ ) was obtained outside the slices. At the end of each experiment, all cells were killed by 24 hour incubation at a low temperature (4°C) and the final PI fluorescence ( $F_{\text{fin}}$ ) was measured. PI uptake was determined by  $(F_i - F_0)/(F_{\text{fin}} - F_0) \times 100$ .

### Assessment of dendrite morphology

Carbocyanine-type membrane tracers were used for labeling cells (Honig and Hume, 1989). A single crystal (~0.1 mm diameter) of the fluorescent carbocyanine dye 1,1'-dioctadecyl 3,3',3'-tetramethylindocarbocyanine perchlorate (DiI) (Molecular Probes) or 3,3'-dipentylloxycarbocyanine iodide (DiO) (Molecular Probes) was inserted into the CA1 and CA3 stratum pyramidale and the stratum granulosum under a stereomicroscope. Some experiments were terminated by fixation with 0.1 M phosphate buffer containing 4% paraformaldehyde at 4°C for 2 hours, at which point DiI was placed directly onto the fixed cultures. After a 2 day incubation at room temperature, dendrite morphology was analyzed using a BioRad MRC-1000 confocal imaging system (BioRad) with a 60 $\times$  objective (Nikon, Tokyo, Japan) and a digital zoom factor of three. Because varicosities had formed almost evenly along dendrites all over the hippocampus (data not shown), the formation of varicosities was quantified along the secondary branch of the apical dendrite of CA1 and CA3 pyramidal cells or along the primary basal dendrite of dentate granule cells.

### Electron microscopy

Culture slices were fixed with 2.5% glutaraldehyde at 37°C for 90 minutes and then fragments of the CA1 region were further fixed with 2%  $\text{OsO}_4$  37°C for 60 minutes. After embedding in Epon, semi-thin sections (0.5  $\mu\text{m}$ ) were stained with toluidine blue for light microscopy and thin sections (70 nm) were stained with uranyl and

lead for micrographs using a Jeol 1200EX electron microscope (JEOL, Inc., Peabody, MA).

### Immunocytochemistry for GluR1

Hippocampal slices were treated with 3  $\mu\text{M}$  NMDA for 10 minutes, then rapidly immersed in ice-cold 4% paraformaldehyde in phosphate-buffered solution (PBS) adjusted to pH 7.4 and fixed for 30 minutes. The slices were then washed three times in PBS, permeabilized with 0.3% Triton X-100 in PBS for 60 minutes at room temperature and then washed again three times in PBS. Some preparations did not receive treatment with Triton X-100 to assess GluR1 on the cell surface. Nonspecific antibody binding was blocked by incubation in 5% horse serum in PBS for 60 minutes at room temperature. The slices were then incubated with the primary antibody, goat polyclonal anti-GluR-1 (Santa Cruz Biotechnology, Santa Cruz, CA), diluted 1:100 in 10% goat serum in PBS overnight at 4°C. This antibody recognizes the extracellular region of the AMPA receptor subunit GluR1 (N-terminal 19 amino acids). The slices were washed three times in PBS and incubated in anti-goat IgG-FITC (Sigma), diluted 1:30 at 4°C for 4 hours. They were then washed again three times in PBS. Images were obtained with a BioRad MRC-1000 confocal imaging system (BioRad). Average fluorescence intensity was estimated by acquiring 8-bit intensity values from 20 different regions (20–400  $\mu\text{m}^2$ ) within the CA1 stratum pyramidale and stratum radiatum.

### Extracellular recording

Cultures were transferred to a recording chamber mounted on a stereoscopic microscope and continuously superfused with warmed (32°C) artificial cerebrospinal fluid consisting of 124 mM NaCl, 26 mM  $\text{NaHCO}_3$ , 10 mM glucose, 5 mM KCl, 1.3 mM  $\text{MgSO}_4$ , 1.24 mM  $\text{KH}_2\text{PO}_4$  and 2.4 mM  $\text{CaCl}_2$ , adjusted to pH 7.4. To record field excitatory postsynaptic potentials (fEPSP), a glass micropipette filled with NaCl (1 M resistance) was placed in the stratum pyramidale of the CA1 region and a bipolar tungsten stimulating electrode was placed along the Schaffer collateral fibers in the CA1 stratum radiatum. The intensity of the stimulation was adjusted to produce

fEPSP with an amplitude of about 50% of maximum. Test stimulations were delivered every 30 seconds (0.033 Hz). NMDA solution (3  $\mu\text{M}$ ) was prepared immediately before use and perfused into the recording chamber for 10 minutes.

### Statistical analysis

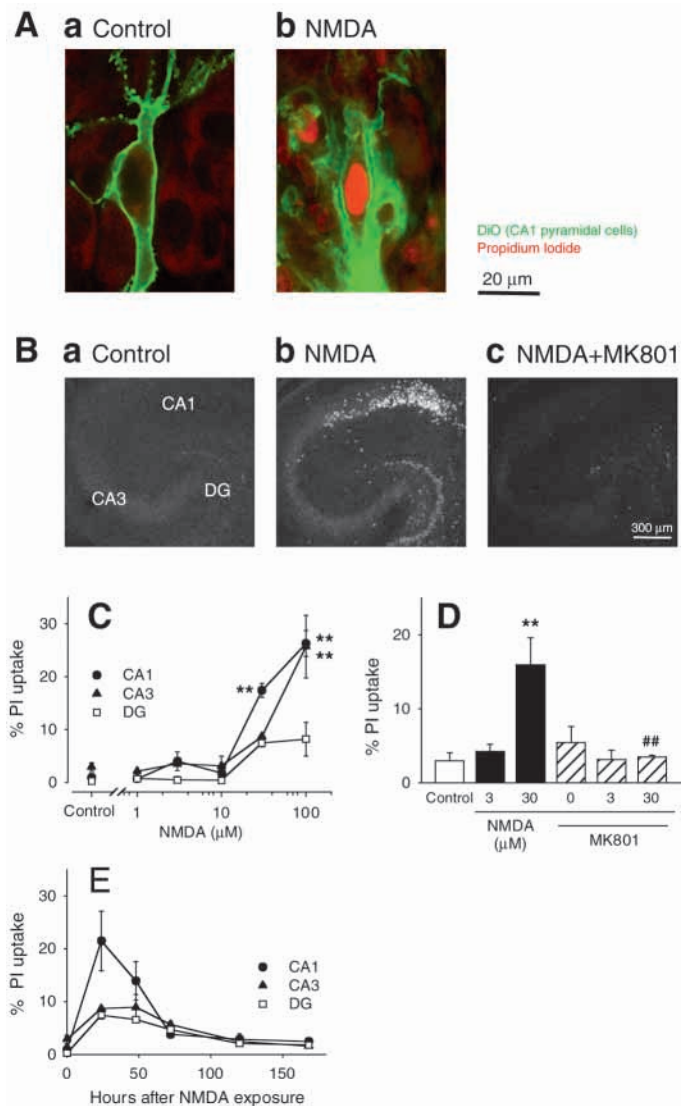
Data are expressed as means  $\pm$  s.e.m. values. Tests of variance homogeneity, normality and distribution were performed to ensure that the assumptions required for standard parametric ANOVA were satisfied. Statistical analysis was performed by Student's *t*-test for two group comparisons of means and one-way or two-way repeated-measures ANOVA and post hoc Tukey's test for multiple pairwise comparisons.

## RESULTS

### NMDA-induced neuronal death

Excessively released excitatory amino acids are well known to ultimately bring about neuronal death (Choi and Rothman, 1990). Thus, to clarify the relationship between dendritic focal swelling and excitotoxic neuronal death, we first characterized the excitotoxicity in organotypic cultures of hippocampal slices.

**Fig. 1.** NMDA induced neuronal cell death in a concentration- and time-dependent manner. (A) Confocal fluorescence micrographs show hippocampal CA1 pyramidal cells double-labeled with DiO (green) and PI (red) 24 hours after 10 minutes exposure to vehicle (a) or 30  $\mu\text{M}$  NMDA (b). The plasma membrane was severely damaged in a PI-positive neuron and thereby the intracellular membrane compartments were also stained with DiO, whereas only the plasma membrane was labeled with DiO in a PI-negative neuron. The faint red signal in the background is derived from an autofluorescence of the cytoplasm of pyramidal neurons. (B) PI fluorescence was imaged in the hippocampal slices 24 hours after 10 minutes exposure to vehicle (a), 30  $\mu\text{M}$  NMDA (b), or a combination of 30  $\mu\text{M}$  NMDA and 10  $\mu\text{M}$  MK-801 (c). (C) Twenty four hours after treatment with NMDA at concentrations in the range of 1–100  $\mu\text{M}$  for 10 minutes, the fluorescence intensity of PI was quantified in each hippocampal subregion, i.e. the CA1 region (circle), the CA3 region (triangle) and the DG (square). Massive neuronal death was observed mainly in the CA1 region at 30  $\mu\text{M}$  NMDA but not evident in any subregions at concentrations of less than 10  $\mu\text{M}$ . (D) NMDA (3 or 30  $\mu\text{M}$ ) was applied for 10 minutes in the absence or presence of 10  $\mu\text{M}$  MK-801. MK-801 was added to culture medium 30 minutes before NMDA exposure. Twenty four hours after NMDA exposure, PI fluorescence was measured in the CA1 region. NMDA-induced neuronal death was prevented by MK-801. (E) PI fluorescence intensities in the CA1 region (circle), the CA3 region (triangle) and the DG (square) were measured 0, 24, 48, 72, 120 or 168 hours after 10 minutes exposure to 30  $\mu\text{M}$  NMDA. Cell death was detected only at 24 and 48 hours. \*\* $P < 0.01$  versus Control, ### $P < 0.01$  versus 30  $\mu\text{M}$  NMDA. Data are the means  $\pm$  s.e.m. of eight to ten slices.



Cultures were exposed to 30  $\mu\text{M}$  NMDA for 10 minutes, and then kept at 37°C for 24 hours. A damaged pyramidal cell in the CA1 region was visualized by labeling with DiO and PI. Confocal microscopic studies demonstrated that DiO did not stay confined to the surface membrane of the neuron but reached internal organelles, presumably the mitochondria, the endoplasmic reticulum, and the nuclear membrane (Fig. 1Ab), whereas only the plasma membrane was labeled in an intact cell (Fig. 1Aa), suggesting that the plasma membrane was severely degenerated in the dying neuron. Indeed, the nuclei in such neurons were always labeled with PI, whereas living neurons had PI-negative nuclei (Fig. 1A). Measurement of fluorescence intensity of PI was therefore used in the following experiments to analyze neuronal death quantitatively. Representative confocal PI images at low magnification are shown in Fig. 1B.

NMDA-induced neuronal death was strictly concentration dependent and regionally specific. NMDA at a concentration of 100  $\mu\text{M}$  severely damaged CA1 and CA3 neurons but DG neurons were relatively resistant to the toxicity (Fig. 1C). NMDA at 30  $\mu\text{M}$  injured mainly the CA1 neurons (Fig. 1Bb,C). Lower concentrations of NMDA (1-10  $\mu\text{M}$ ) did not induce apparent cell death in any hippocampal subregions (Fig. 1C). NMDA toxicity was effectively blocked by the noncompetitive NMDA receptor antagonist MK-801 (Fig. 1Bc,D), and almost completely disappeared when NMDA was applied in  $\text{Ca}^{2+}$ -free culture medium (data not shown).

NMDA-induced neuronal death also exhibited temporal dependence. Following a 10 minute exposure to 30  $\mu\text{M}$  NMDA, an increase in PI uptake occurred after 24 to 48 hours, whereas no significant PI uptake was detected immediately after exposure. Thereafter, PI signals gradually decreased to baseline, which may represent a decrease in the number of neuronal corpses, probably via phagocytosis by surrounding microglial cells. These data suggest that the NMDA toxicity emerged in a delayed, relatively narrow time window.

### NMDA-induced dendritic focal swelling

NMDA receptors tend to be localized in postsynaptic neuronal dendrites (Racca et al., 2000). The dendrite is therefore assumed to be particularly vulnerable to NMDA injury and thus to convey the NMDA-induced damage to the soma. To evaluate the early stages of NMDA toxicity, we examined the acute effects of NMDA on dendritic morphology in hippocampal slice cultures.

Neuronal morphology was visualized using the fluorescent membrane tracer DiI. When cultures were exposed to 30  $\mu\text{M}$  NMDA for 10 minutes, there was widespread appearance of regions of alternating dilatation and constriction along the length of the dendrites (Fig. 2A; Fig. 7Ab). Initially some, but not all, dendritic spines underwent retraction and eventually disappeared within 1-2 minutes of exposure. Simultaneously, mild focal swellings (varicosities) appeared, but did not replace dendritic spines because the varicosities occasionally bore a few spines on their surface. The varicosities gradually grew larger, and formed segmental focal swelling moniliformly along the

length of the dendrites within 5 minutes of exposure. Following washout of NMDA, the varicosity beading remained for at least 60 minutes (Fig. 2A), which suggests that varicosity formation is a rapid, long-lasting change in dendritic structure.

Electron microscopic analysis revealed ultrastructural alterations associated with the varicosity (Fig. 2B). Varicosities were typically 4-10  $\mu\text{m}$  in length and 2-8  $\mu\text{m}$  in diameter, and separated by narrow cytoplasmic segments 0.1-1.3  $\mu\text{m}$  in diameter and 1.5-7  $\mu\text{m}$  in length. The cytoplasm of varicosities contained clear vacuoles and many short fragments of cytoskeletal elements. The region between varicosities contained few organelles. The microtubules within these segments were tightly packed, arranged longitudinally, and appeared to be continuous.

Concentration-dependence of NMDA-induced varicosity formation was evaluated immediately after a 10 minute application. Increasing concentrations of NMDA reduced the density of spines along the length of the dendrites (Fig. 3Aa). By contrast, the ratio of varicosity-bearing dendrites (Fig. 3Ab), the density of varicosities along the length of dendrites (Fig. 3Ac) and the average size of varicosities (Fig. 3Ad) increased in a concentration-dependent manner. In contrast to

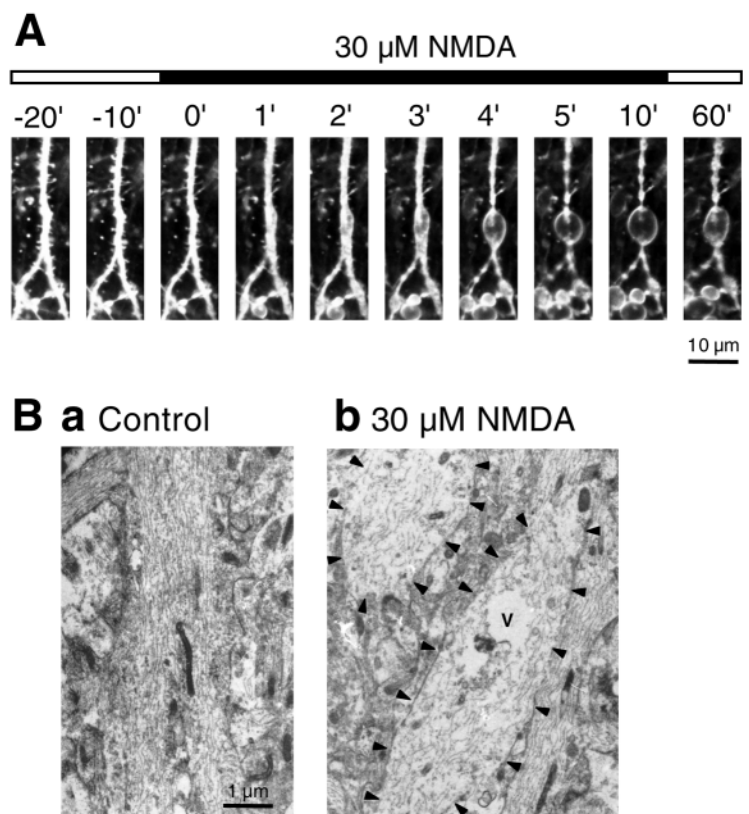


**Fig. 2.** Rapid formation of dendritic focal swelling in response to NMDA exposure. (A) Time-lapse confocal images of an apical dendrite of DiI-labeled CA1 pyramidal neuron following 10 minutes exposure to 30  $\mu\text{M}$  NMDA. Numbers above the images indicate time (minutes) after NMDA treatment. NMDA induced a decrease in the number of spines and subsequently produced focal swelling along the dendrites. (B) Electron micrograph of varicosities in apical dendrites of DiI-labeled CA1 pyramidal neurons in untreated (a) and NMDA-treated (30  $\mu\text{M}$ , 10 minutes) (b) slices. The varicosities, indicated by arrowheads, contained clear vacuoles (V) and many short fragments of degenerated microtubules.

NMDA-induced neuronal death, no regional difference was detected in the dendrite swelling, and varicosity formation was observed in the CA1 region, the CA3 region and the DG. Moreover, the concentration of NMDA required to produce apparent dendritic beadings was approximately 3  $\mu\text{M}$ , which was ten times less than that required to evoke neuronal cell death.

Time-course analysis confirmed that the varicosity formation was initiated within minutes in response to 3  $\mu\text{M}$  NMDA, and reached maximal formation within 6 minutes of exposure (Fig. 3B). Even after removal of NMDA, the varicosities remained for at least 24 hours, and then gradually resolved spontaneously (Fig. 3B). This time-response curve was observed almost equally in the CA1 region, the CA3 region and the DG. Varicosity formation was completely blocked by MK-801 (Fig. 3C). Taken together, the data suggest that NMDA receptor-mediated varicosity formation is rapid, widespread, long-lasting and reversible.

**Production of dendritic varicosity by nontoxic stimulants**

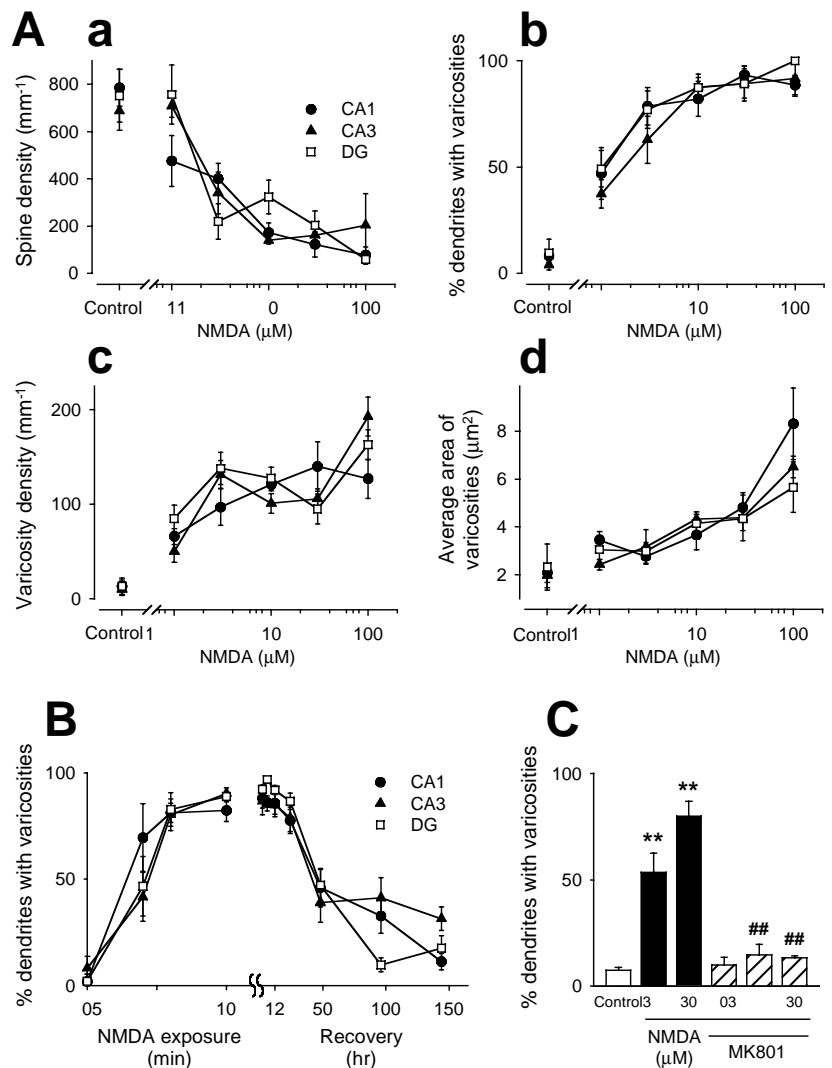
To further elucidate the relationship between neuronal death and varicosity formation, we examined the effects of the non-NMDA receptor agonists kainate and AMPA. Application of kainate invoked neuronal death selectively in the CA3 region at concentrations in the range of 100-300  $\mu\text{M}$ , whereas it produced varicosities in all hippocampal

subregions even at a low concentration of 30  $\mu\text{M}$  (Fig. 4A). Similarly, AMPA elicited neuronal death mainly in the CA1 and CA3 regions at higher concentrations (100-300  $\mu\text{M}$ ), whereas it yielded focal swellings throughout the hippocampus even at a low concentration of 30  $\mu\text{M}$  (Fig. 4B). Varicosity formation was therefore induced by sublethal stimulation.

In addition, we found many other stimulants that produced neurite beading without inducing neuronal death. First, the voltage-sensitive  $\text{Na}^+$  channel activator veratridine effectively evoked varicosity formation within 10 minutes, but did not increase PI uptake (Fig. 4C). Interestingly, when hippocampal slices were incubated in  $\text{Ca}^{2+}$ -free solution for 30 minutes without exposure to any chemical stimulants, dendritic varicosities appeared spontaneously (Fig. 4C). Incubation in  $\text{Ca}^{2+}$ -free solution per se did not elicit neuronal death. Incidentally, NMDA-induced varicosity formation was not inhibited in  $\text{Ca}^{2+}$ -free medium (data not shown). It is therefore likely that  $\text{Ca}^{2+}$  is not required for varicosity formation, but rather prevents the manifestation of focal swelling in dendrites.

Following a 12 hour exposure to the microtubule-depolymerizing agent colchicine, varicosities emerged spontaneously (Fig. 4Cb). The same treatment did not induce neuronal death in the CA1 or CA3 region (Fig. 4Ca), although

**Fig. 3.** Characterization of NMDA-induced morphological changes in dendrites. (A) Immediately after 10 minutes exposure to NMDA at concentrations in the range of 1-100  $\mu\text{M}$ , slices were fixed with 4% paraformaldehyde and the dendrites were labeled with DiI. The density of spines along the length of the dendrites (a), the percentage of dendrites bearing varicosities (b), the density of varicosities along the dendrites (c) and the average size of varicosities (d) were measured. NMDA treatment resulted in a reduction in the spine density and simultaneously caused an increase in the number and size of varicosities in a concentration-dependent manner. No regional difference in these morphological changes was detected among the CA1 region (circle), the CA3 region (triangle) and the DG (square). (B) Slice cultures were fixed after 4, 6 and 10 minutes of NMDA exposure, or at 6, 12, 24, 48, 96 and 144 hours after 10 minute exposure to 3  $\mu\text{M}$  NMDA and the ratio of varicosity-bearing dendrites was measured. The dendritic varicosities appeared within 4 minutes of exposure and were observed in about 80% of dendrites by 6 minutes of exposure, but gradually decreased until 144 hours after removal of NMDA. (C) NMDA (3 or 30  $\mu\text{M}$ ) was applied for 10 minutes in the absence or presence of 10  $\mu\text{M}$  MK-801. Immediately, the cultures were fixed and the ratio of dendrites with varicosities was measured in the CA1 region. MK-801 was added to culture medium 30 minutes before NMDA exposure. NMDA-induced varicosity formation was almost completely prevented by MK-801.  $**P < 0.01$  versus Control,  $##P < 0.01$  versus slices treated with corresponding doses of NMDA. Data are the means  $\pm$  s.e.m. of 9-12 slices.



the DG neurons were severely damaged (data not shown). Similar results were obtained for another microtubule-depolymerizing agent, nocodazole (data not shown). Likewise, the actin-depolymerizing agents cytochalasin D and latrunculin A induced dendritic beading but did not produce neuronal death (Fig. 4C). Taken together, these results show that there is a large number of nontoxic stimulants that can produce dendritic varicosities, suggesting that the varicosity formation per se does not contribute causally to neuronal injury.

Despite the established theory that  $\text{Ca}^{2+}$  is essential for triggering neuronal death (Choi, 1992), varicosity formation was virtually independent of  $\text{Ca}^{2+}$ . Rather,  $\text{Ca}^{2+}$ -free conditions promoted dendrite swelling. In addition, NMDA-induced varicosity formation was rapid and reversible, and the time course of the swelling and its recovery corresponded to the time window for neuronal death. Furthermore, the concentrations of excitotoxin required to produce varicosity were considerably lower than those required for neuronal death. These observations prompted us to explore the possibility that the formation of varicosities is, rather, a self-protective response against excitotoxicity.

### Pathophysiological consequences of varicosity formation

A number of studies indicate that posts ischemic blockade of the AMPA receptor is sufficient to mitigate neuronal damage in experimental ischemic models (Sheardown et al., 1990; Nelligard and Wieloch, 1992), suggesting that ischemic excitotoxicity is attributable to ischemia-induced changes in the control mechanisms of AMPA receptor-coupled processes or to changes in AMPA receptor characteristics. Furthermore, recent studies on synaptic plasticity show that NMDA receptor activity regulates the function and cellular distribution of AMPA receptors (Malenka and Nicoll, 1999).

To determine whether exogenously applied NMDA affects the cellular localization of AMPA receptors in hippocampal slice cultures, slices treated with 3  $\mu\text{M}$  NMDA for 10 minutes were immunostained with antibody against the major subunit of AMPA receptor GluR1 (Fig. 5). This antibody recognizes the extracellular domain of GluR1. We were thus able to distinguish between receptors expressed on the cell surface and intracellular receptors under nonpermeant and permeant conditions. Although total GluR1 immunoreactivity was evident throughout the hippocampus, the cell-surface GluR1 was distributed predominantly in the stratum radiatum. Brief NMDA exposure resulted in a reduction in cell-surface GluR1 in the stratum radiatum without affecting the total number of GluR1 (Fig. 5). This result indicates that NMDA receptor activation decreased a proportion of the surface GluR1, probably via promoting AMPA receptor internalization. By contrast, the distribution of

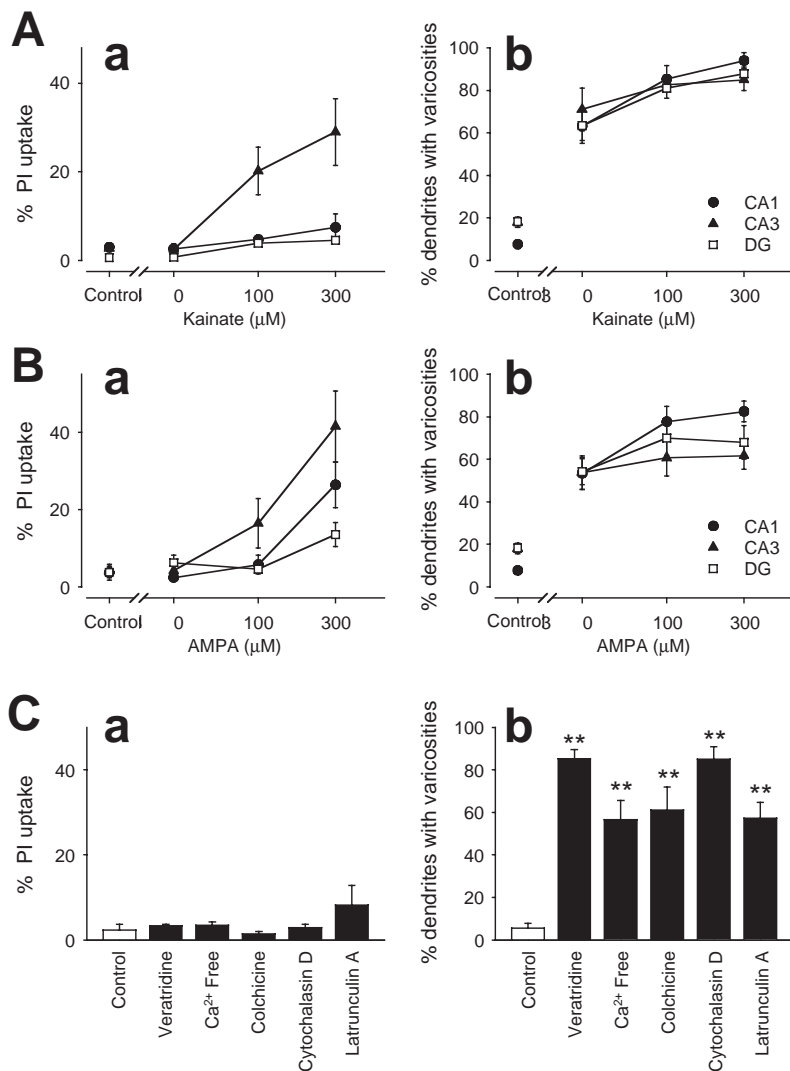
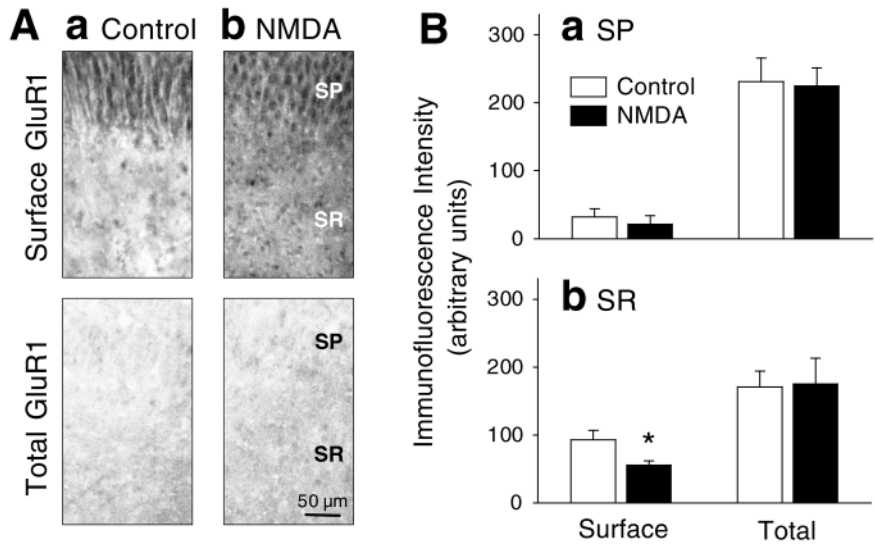


**Fig. 4.** Discrepancies between neuronal death and dendritic varicosity formation. Slices were treated with kainate (A), AMPA (B) or other drugs (C). Kainate, AMPA and veratridine (10  $\mu\text{M}$ ) were applied for 10 minutes.  $\text{Ca}^{2+}$ -free buffer was applied for 30 minutes. Colchicine (100  $\mu\text{M}$ ), cytochalasin D (1  $\mu\text{M}$ ) and latrunculin A (1  $\mu\text{M}$ ) were applied for 12 hours. The cultures were divided into two groups: one group was cultivated at 37°C for 24 hours and PI uptake was measured (a), and the other group was immediately fixed with 4% paraformaldehyde and the ratio of dendrites bearing varicosities was measured (b). Panel C shows values in the CA1 region. Varicosity formation was induced by various stimulants, even at low concentrations that did not give rise to cell death. \*\* $P < 0.01$  versus Control. Data represent the means  $\pm$  s.e.m. of 9–13 slices.

GluR1 in the stratum pyramidale was almost unaffected by NMDA exposure, which suggests that AMPA receptor internalization is a dendrite-specific event.

On the basis of this observation, we conducted an electrophysiological analysis to investigate whether synaptic transmission is affected by NMDA exposure. The stratum radiatum of the CA1 region was stimulated, and the fEPSP was recorded from the CA1 stratum pyramidale. This synaptic response reflects mainly AMPA-mediated neurotransmission, being completely blocked by 10  $\mu\text{M}$  6-cyano-7-nitroquinoxaline-2,3-dione, a non-NMDA receptor antagonist (data not shown). The fEPSP was markedly reduced

**Fig. 5.** NMDA-induced depletion of cell-surface AMPA receptors. Slices were treated with 3  $\mu$ M NMDA for 10 minutes and immediately fixed with 4% paraformaldehyde and then the immunohistochemical localization of the GluR1 subunit was analyzed with a confocal microscope. (A) Representative confocal sections through the CA1 stratum pyramidale (SP) and the stratum radiatum (SR) show the cellular distribution of GluR1. AMPA receptors containing GluR1 on the cell surface were labeled with antibody under nonpermeant conditions (Surface GluR1) and the total GluR1 population was probed under permeant conditions (Total GluR1). (B) NMDA-induced reduction of cell-surface GluR1 was assessed in the CA1 stratum pyramidale (a) and the CA1 stratum radiatum (b) by using quantitative colorimetric assay. NMDA induced a decrease in cell-surface GluR1 subunits (Surface) without affecting the total number of GluR1 (Total), resulting in a lower proportion of surface AMPA receptors. The GluR1 internalization was predominantly observed in the dendrite-rich area (SR), as compared with the soma-rich zone (SP). \* $P < 0.05$  versus Control. Data represent the means  $\pm$  s.e.m. of eight slices.



immediately after bath application of 3  $\mu$ M NMDA, and stabilized at a level of about 30% of control values within 2-3 minutes (Fig. 6A). Even 24 hours after removal of NMDA, fEPSP amplitudes remained depressed, but had recovered to near pretreatment levels by 48 hours (Fig. 6B). Interestingly, this time course corresponds with the recovery time observed for varicosities.

Taken together, NMDA induced a rapid, long-lasting depression of AMPA-mediated synaptic function. Considering that excessive AMPA receptor activation after ischemic injury may cause neurotoxicity (Sheardown et al., 1990; Nelligard and Wieloch, 1992), these results support our hypothesis that

dendritic varicosity formation may represent an early defensive response against excitotoxicity.

**Excitotoxicity aggravation due to inhibition of varicosity formation**

The final set of experiments aimed to determine whether or not inhibition of varicosity formation affects neuronal death. If varicosity formation serves as a defensive response against excitotoxicity, neurons will be severely damaged if they cannot do this efficiently. Thus, we searched for strategies to prevent varicosity formation. (Fig. 7).

In cultured cortical neurons, Hasbani et al. (Hasbani et al., 1998) have already shown that varicosity formation in response to NMDA is substantially attenuated in reduced Na<sup>+</sup> buffer. Therefore, we first examined whether low Na<sup>+</sup> conditions inhibit varicosity formation in organotypic cultures of hippocampal slices. Na<sup>+</sup> concentration was reduced from 150 mM to 30 mM by iso-osmotic substitution of Na<sup>+</sup> with choline. We confirmed that NMDA did not induce varicosity formation in low Na<sup>+</sup> solution, and that exposure to low Na<sup>+</sup> buffer alone did not affect dendrite morphology (Fig. 7Ac,B). These results suggest that Na<sup>+</sup> entry is required for varicosity formation. Therefore, we next investigated the effect of the voltage-

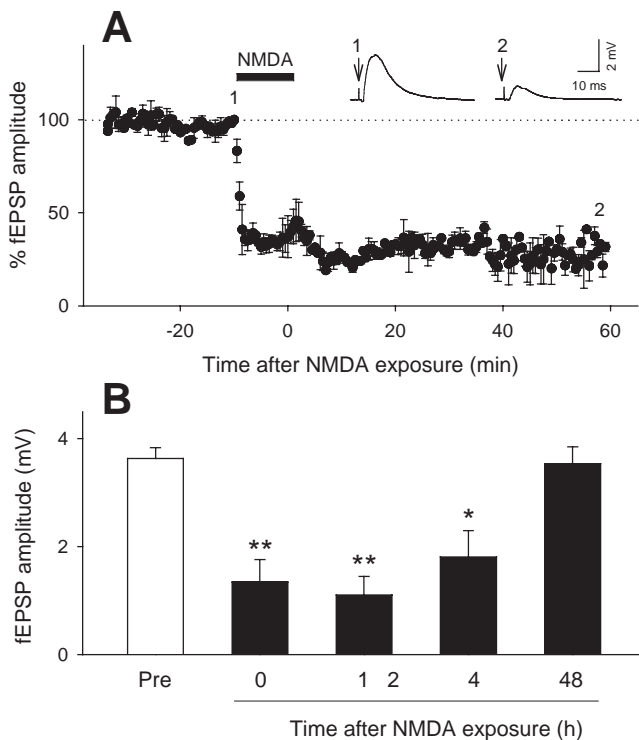


**Fig. 6.** Rapid, long-lasting depression of synaptic transmission following NMDA exposure. (A) Time course of changes in fEPSP amplitude following a 10 minute bath application of 3  $\mu$ M NMDA. fEPSP evoked by stimulation of the Schaffer collaterals was recorded extracellularly from the CA1 stratum pyramidale of cultured hippocampal slices. Representative fEPSP recordings at times -10 (1) and 58 (2) are shown in the inset. Arrows indicate stimulation-elicited artifacts. Data are expressed as the percentage of pretreatment fEPSP amplitude; means  $\pm$  s.e.m. of four slices. (B) Reversible NMDA-induced suppression of synaptic transmission. fEPSP was recorded immediately before (pre) or at 0, 1, 24 and 48 hours after 10 minutes exposure to 3  $\mu$ M NMDA. Data are the means  $\pm$  s.e.m. of seven to eight different slices. \* $P < 0.05$ , \*\* $P < 0.01$  versus Pre. NMDA induced a rapid, long-lasting decrease in synaptic response, which almost completely recovered after NMDA washout. Recovery time was relatively slow, requiring 48 hours.

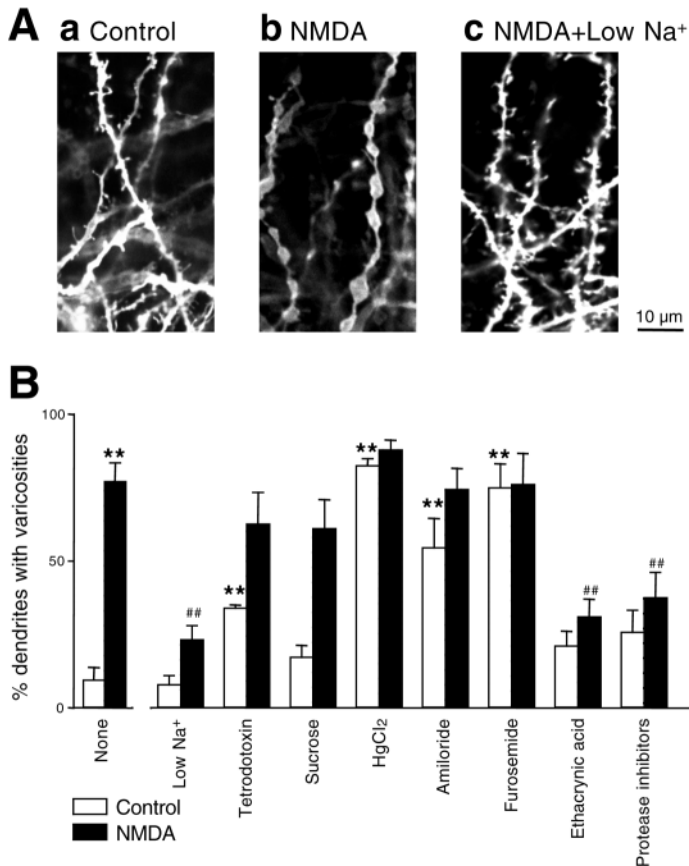


**Fig. 7.** Low Na<sup>+</sup> buffer, ethacrynic acid and protease inhibitors prevent NMDA-induced dendritic varicosity formation. (A) Representative confocal images of dendrites of CA1 pyramidal cells in untreated slices (a) or 30  $\mu$ M NMDA-treated slices in normal (b) or low Na<sup>+</sup> solution (c). Culture medium was changed to low Na<sup>+</sup> buffer 30 minutes before 10 minutes exposure to NMDA. No varicosity was generated under low Na<sup>+</sup> conditions. (B) Effects of various manipulations and drugs on NMDA-induced varicosity formation. The culture medium was changed to lowered Na<sup>+</sup> solution or 200 mM sucrose-containing (hyperosmotic) medium 30 minutes before NMDA exposure. Tetrodotoxin (1  $\mu$ M), HgCl<sub>2</sub> (100  $\mu$ M), amiloride (100  $\mu$ M), furosemide (100  $\mu$ M) and ethacrynic acid (400  $\mu$ M) were added 30 minutes before NMDA exposure. A mixture of protease inhibitors (1:1000) was applied 12 hours prior to NMDA exposure. Slices received 10 minutes treatment with 0  $\mu$ M (open columns) or 30  $\mu$ M NMDA (filled columns), immediately followed by fixation with 4% paraformaldehyde. Low Na<sup>+</sup> buffer, ethacrynic acid and protease inhibitors significantly blocked the varicosity formation, whereas tetrodotoxin, amiloride and furosemide induced varicosity formation. Data are expressed as the means  $\pm$  s.e.m. of 9–12 slices. \*\* $P$ <0.01 versus intact slices (None and Control), ## $P$ <0.01 versus NMDA alone (None and NMDA).

sensitive Na<sup>+</sup> channel blocker tetrodotoxin on NMDA-induced varicosity formation. We found tetrodotoxin to be virtually ineffective against this form of dendrite swelling (Fig. 7B), although the same treatment attenuated veratridine-induced varicosity formation (data not shown). Rather, tetrodotoxin alone slightly induced spontaneous dendritic focal swelling. Nonetheless, these results indicate that dendrite swelling is dependent on ionic flow.

We next investigated the effect of hyperosmotic conditions on NMDA-induced varicosity formation. Hypertonic solution was prepared by supplementation with 200 mM sucrose. However, the high osmotic conditions did not affect the focal swelling (Fig. 7B). Furthermore, the effects of the broad inhibitor of water channel aquaporins (except AQP4) HgCl<sub>2</sub>, the Na<sup>+</sup>/H<sup>+</sup> exchanger inhibitor amiloride, and the Na<sup>+</sup>,K<sup>+</sup>,2Cl<sup>-</sup> cotransporter inhibitor furosemide were examined, but none of them blocked varicosity formation (Fig. 7B). Rather, all three inhibitors produced severe dendritic varicosity beading. However, the HCO<sub>3</sub><sup>-</sup>/Cl<sup>-</sup> exchanger inhibitor ethacrynic acid significantly prevented NMDA-induced varicosity formation (Fig. 7B).

Electron microscopic analysis revealed that varicosities contained large numbers of cleavages of cytoskeletal elements, suggesting that dendrite swelling is associated with cytoskeletal protein degradation, conceivably via a proteolytic process. We therefore evaluated the effect of protease inhibitors. When NMDA was co-applied with a protease inhibitor cocktail containing 100  $\mu$ M 4-(2-aminoethyl)-benzylsulfonyl fluoride, 80 nM aprotinin, 5  $\mu$ M bestatin, 1.5  $\mu$ M E-64, 2  $\mu$ M leupeptin and 1  $\mu$ M pepstatin, varicosity formation was significantly attenuated (Fig. 7B).

On the basis of these observations, we were able to assess the effect of low Na<sup>+</sup> conditions and protease inhibitors, both of which efficiently prevented NMDA-induced varicosity formation, on NMDA-induced neuronal death. Either low Na<sup>+</sup> conditions or pretreatment with protease inhibitors actually exacerbated NMDA excitotoxicity (Fig. 8). Two observations were of particular importance here. First, NMDA induced neuronal death not only in the CA1 regions but also in the CA3 region and the DG. Second, NMDA caused neuronal death even at concentrations too low to induce neuronal death under normal conditions. Ethacrynic acid produced similar results; when 3  $\mu$ M NMDA was applied in the presence of 400  $\mu$ M ethacrynic acid, massive cell death occurred all over the hippocampus (data not shown).

We determined whether NMDA treatment in reduced Na<sup>+</sup> solution elicits a long-lasting depression of synaptic transmission. When the bath solution was changed to low Na<sup>+</sup> buffer, fEPSP amplitudes were transiently facilitated within the first minute, immediately followed by a gradual decline, with the synaptic responses almost disappearing within 10 minutes (Fig. 9). However, synaptic response fully recovered within 30 minutes after replacement with normal Na<sup>+</sup> solution. When 3  $\mu$ M NMDA was applied for 10 minutes in low Na<sup>+</sup> solution, fEPSP amplitudes were not depressed but rather slightly enhanced (Fig. 9). No statistically significant difference in fEPSP amplitudes at 90 minutes after washout was detected between untreated and NMDA-treated slices.

## DISCUSSION

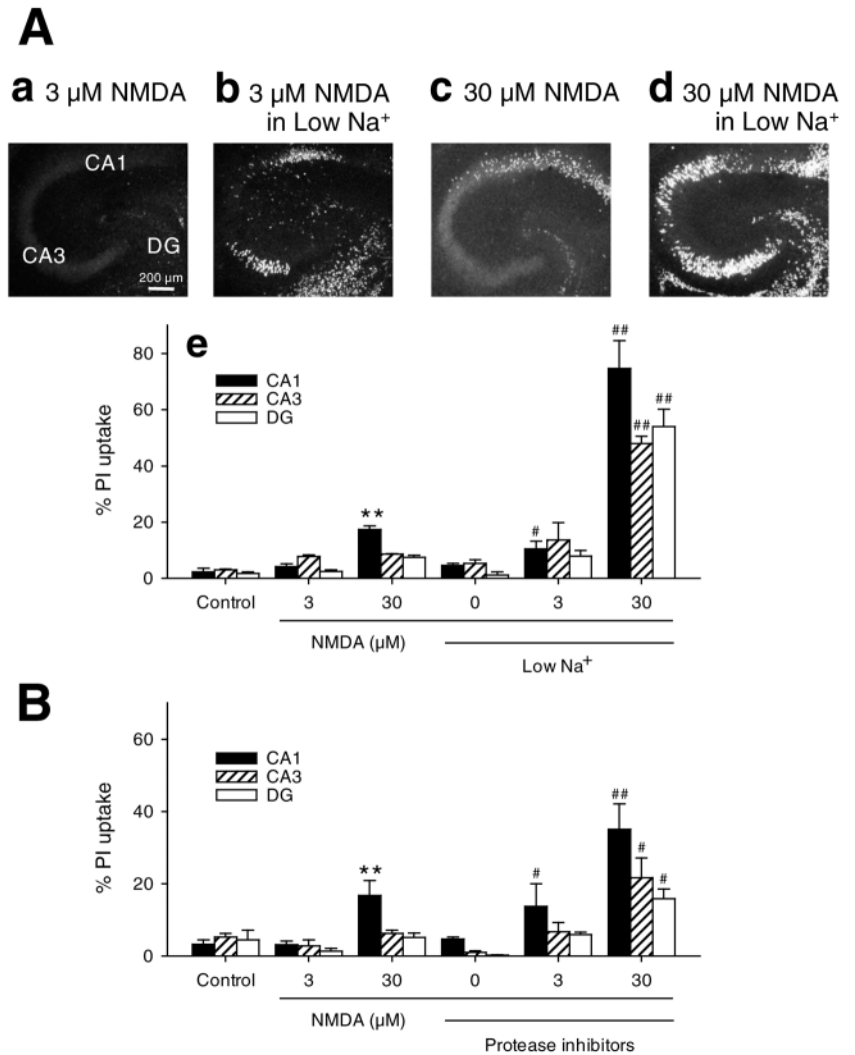
The dendrite serves as a pivotal input device of a neuron, which depends on its specialized, unique geometry - an anatomical framework for spatiotemporal integration of signals from hundreds or thousands of synapses arranged on its complex arbor (Midtgaard, 1994). For this reason, the dendrite may also be a major input site of stressful disturbance under pathological conditions, such as excessive excitatory signals, and thus has

**Fig. 8.** Inhibition of varicosity formation aggravates NMDA-induced neuronal death. (A) Representative confocal images of PI fluorescence in hippocampal slices 24 hours after 10 minutes exposure to 3  $\mu$ M (a,b) or 30  $\mu$ M (c,d) NMDA in normal (a,c) or low  $\text{Na}^+$  conditions (b,d). Culture medium was changed to normal or low  $\text{Na}^+$  buffer 30 minutes prior to NMDA treatment. (e) PI fluorescence intensity was quantified in the CA1 region (solid columns), the CA3 region (hatched columns) and the DG (open columns). Low  $\text{Na}^+$  conditions exacerbated NMDA excitotoxicity; NMDA in low  $\text{Na}^+$  solution evoked neuronal death all over the hippocampus. Note that treatment with NMDA even at a concentration of 3  $\mu$ M showed apparent neurotoxicity. (B) Slices were treated with a mixture of protease inhibitors (1:1000) for 12 hours and exposed to 3 or 30  $\mu$ M NMDA. They were subsequently incubated in normal medium at 37°C for 24 hours and PI uptake was measured. Treatment with protease inhibitors exacerbated NMDA-induced neuronal death. \*\* $P < 0.01$  versus Control, # $P < 0.05$ , ## $P < 0.01$  versus corresponding concentrations of NMDA. Data are the means  $\pm$  s.e.m. of 9–12 slices.

been considered to be highly vulnerable to neuronal injury as compared with the axon and the soma. Indeed, diverse types of dendritic injury associated with excitotoxicity have long been illustrated (Ramón y Cajal, 1909; Olney, 1971; Ikonomidou et al., 1989). The present study also demonstrated several morphological and physiological alterations in response to NMDA receptor activation, including a loss of spines, dendritic focal swelling, cytoskeletal degradation and a depression of neurotransmission. Indeed, it is possible for all of these phenomena to contribute to a collapse of normal neuron function.

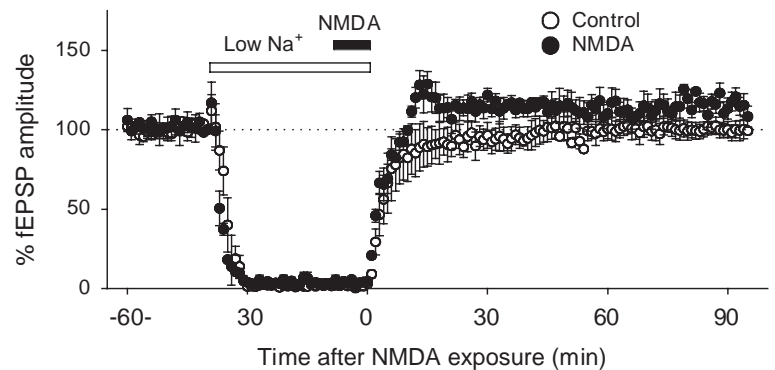
Our evaluation, however, of the relationship between dendritic injury and subsequent neuronal death revealed that the two phenomena are separable and involve distinct mechanisms. Importantly, the formation of varicosities was rapid and reversible, and accompanied by AMPA receptor internalization and a rapid, long-lasting depression in synaptic transmission. Considering that prolonged excessive AMPA receptor activity following NMDA receptor activation is likely to be a causal factor in inducing delayed neuronal death in excitotoxicity (Sheardown et al., 1990; Nellygard and Wieloch,

**Fig. 9.** Lack of effect of NMDA on synaptic transmission in low  $\text{Na}^+$  solution. When  $\text{Na}^+$  concentration of the bath solution was reduced from 150 mM to 30 mM, fEPSP amplitudes dropped markedly within 10 minutes, but completely recovered within 30 minutes after application of basal  $\text{Na}^+$  concentration (open circles). Bath application of 3  $\mu$ M NMDA for 10 minutes did not cause depression of fEPSP amplitudes in low  $\text{Na}^+$  solution (closed circles). Data are expressed as a percentage of baseline fEPSP amplitude (at time -40); means  $\pm$  s.e.m. of four slices.



1992), the dendrite swelling and AMPA receptor inactivation may represent an early, self-protective response against excitotoxicity. This idea is further supported by the fact that treatments preventing the manifestation of focal swelling cause a significantly greater level of neuronal cell death in excitotoxicity.

Although neuronal death and varicosity formation were both triggered by NMDA receptor activation, their ionic dependence was distinct, which suggests that they are mediated by independent cellular mechanisms. The former was dependent



on  $\text{Ca}^{2+}$ , and the latter required  $\text{Na}^+$ . Although it is well known that excitotoxin-induced neuronal death is initiated by excessive  $\text{Ca}^{2+}$  influx through NMDA receptor channels (Choi, 1992), very little is known about the role of  $\text{Na}^+$  in dendrite swelling. Veratridine application alone caused segmental neurite beading, and the veratridine-induced varicosity formation was prevented by tetrodotoxin. Therefore,  $\text{Na}^+$  entry is sufficient, and hence may be the primary event in this type of swelling. However, tetrodotoxin did not affect NMDA-induced dendritic beading, which suggests that NMDA receptor-dependent swelling does not require  $\text{Na}^+$  influx through tetrodotoxin-sensitive  $\text{Na}^+$  channels. Several reports show that cell volume is regulated by the  $\text{Na}^+/\text{H}^+$  exchanger and  $\text{Na}^+,\text{K}^+,\text{2Cl}^-$  cotransporter in various types of cells such as red blood cells, ovary cells and CHO cells (Sarkadi et al., 1984; Parker, 1988; McCarty and O'Neil, 1992). These observations raise the possibility that such transporters are candidates for a route of  $\text{Na}^+$  entry in NMDA-induced varicosity formation. However, both amiloride and furosemide were virtually ineffective in preventing dendrite swelling. Therefore, we believe that it is the  $\text{Na}^+$  influx through the NMDA receptor channel itself that mediates the dendrite focal swelling. In this context, NMDA receptor activation stimulates two distinct signaling pathways in neurons:  $\text{Ca}^{2+}$  activates various  $\text{Ca}^{2+}$ -dependent enzymes, including kinases and proteases, and may cause eventual neuronal death, and  $\text{Na}^+$  induces dendritic focal swellings. Although Yu and Salter (Yu and Salter, 1998) suggested that  $\text{Na}^+$  influx through the NMDA receptor activates the protein kinase Src,  $\text{Na}^+$ -activated signaling molecules that mediate varicosity formation or cell swelling have not been identified. Therefore, it is interesting that protease inhibitors diminished NMDA-induced varicosity formation.  $\text{Na}^+$ -activated proteases may be involved in varicosity formation.

In the context of synaptic plasticity, it is also interesting that prolonged NMDA exposure induced a long-lasting depression of synaptic transmission. The synapses of the hippocampus are well known to display a long-lasting increase and decrease in strength of synaptic communication following repetitive synaptic activation. This phenomenon is termed long-term potentiation (LTP) and long-term depression (LTD), respectively, and is considered to be the primary experimental model for investigating the cellular basis of learning and memory in vertebrates (Malenka and Nicoll, 1999). Induction of LTP and LTD is generally believed to depend on NMDA receptor activation. Indeed, using acute hippocampal slice preparations, Lee et al. (Lee et al., 1998) indicated that bath application of NMDA (20  $\mu\text{M}$ , 3 minutes) induces LTD and dephosphorylation of the GluR1 subunit at serine 845. Other evidence shows that, in primary cultures of hippocampal neurons, a brief application of 100  $\mu\text{M}$  glutamate results in a rapid decrease in the frequency of miniature EPSCs, and induces GluR1 redistribution away from synaptic sites, without causing neurotoxicity (Lissin et al., 1999). Furthermore, Man et al. (Man et al., 2000) recently suggested that LTD involves clathrin-dependent AMPA receptor internalization. Consistent with these observations, we demonstrated that GluR1 internalization and long-lasting depression in synaptic transmission were associated with NMDA-induced varicosity formation. Therefore, it is possible that these dendritic changes under pathological conditions involve a common molecular

mechanism for synaptic plasticity. If this is true, it is intriguing to find that NMDA-induced synaptic depression was completely abolished in reduced  $\text{Na}^+$  solution. To our knowledge, there has not yet been an indication of a  $\text{Na}^+$  requirement in the induction of hippocampal LTP or LTD, whereas  $\text{Na}^+$  influx through AMPA receptor channels is critical for the induction of LTD in cerebellar Purkinje neurons (Linden et al., 1993). Very recently, Rose and Konnerth (Rose and Konnerth, 2001) reported that LTP induction protocol elicits an increase in intracellular  $\text{Na}^+$  levels via NMDA receptor channels. Thus, clarifying a  $\text{Na}^+$ -activated signaling pathway may provide a new insight into long-lasting changes in synaptic efficacy in both physiological and pathological cases.

In conclusion, selective dendrite changes in shape and function are among the earliest signs of excitotoxic injury, and observed in diverse neurological diseases and neurodegenerative disorders. For years, these pathologic changes have been thought as a prelude to eventual cell death (Olney, 1971). Indeed, as shown in the present study, they may distort neuronal functions. However, these alterations are transient and fully reversible. In long time scales, therefore, they are not causally associated with neuronal injury. Thus, we prefer the hypothesis that NMDA-induced paralysis of synaptic function and morphological changes in dendrites serve as a safety device against excessive stimulation of glutamate receptors. Elucidating mechanisms that mediate the dendritic alterations under pathological conditions may be of fundamental importance to understanding mechanisms of neuronal injury.

This work was supported by Grants-in-aid for scientific research from the Ministry of Education, Science and Culture of Japan. We thank Michael Critchley for his critical review of this manuscript, and Maki Kobayashi-Yamada for her assistance with the manuscript preparation.

## REFERENCES

- Al-Noori, S. and Swann, J. W. (2000). A role for sodium and chloride in kainic acid-induced beading of inhibitory interneuron dendrites. *Neuroscience* **101**, 337-348.
- Bindokas, V. P. and Miller, R. J. (1995). Excitotoxic degeneration is initiated at non-random sites in cultured rat cerebellar neurons. *J. Neurosci.* **15**, 6999-7011.
- Bittigau, P. and Ikonomidou, C. (1997). Glutamate in neurologic diseases. *J. Child. Neurol.* **12**, 471-485.
- Buchs, P. A. and Muller, D. (1996). Induction of long-term potentiation is associated with major ultrastructural changes of activated synapses. *Proc. Natl. Acad. Sci. USA* **93**, 8040-8045.
- Choi, D. W. (1992). Excitotoxic cell death. *J. Neurobiol.* **23**, 1261-1276.
- Choi, D. W. and Rothman, S. M. (1990). The role of glutamate neurotoxicity in hypoxic-ischemic neuronal death. *Annu. Rev. Neurosci.* **13**, 171-182.
- Coyle, J. T. and Puttfarcken, P. (1993). Oxidative stress, glutamate, and neurodegenerative disorders. *Science* **262**, 689-695.
- Hasbani, M. J., Hyrc, K. L., Faddis, B. T., Romano, C. and Goldberg, M. P. (1998). Distinct roles for sodium, chloride, and calcium in excitotoxic dendritic injury and recovery. *Exp. Neurol.* **154**, 241-258.
- Honig, M. G. and Hume, R. I. (1989). Dil and DiO: versatile fluorescent dyes for neuronal labelling and pathway tracing. *Trends Neurosci.* **12**, 333-341.
- Hori, N. and Carpenter, D. O. (1994). Functional and morphological changes induced by transient in vivo ischemia. *Exp. Neurol.* **129**, 279-289.
- Ikegaya, Y. (1999). Abnormal targeting of developing hippocampal mossy fibers after epileptiform activities via L-type  $\text{Ca}^{2+}$  channel activation in vitro. *J. Neurosci.* **19**, 802-812.

- Ikonomidou, C., Price, M. T., Mosinger, J. L., Friedrich, G., Labruyere, J., Salles, K. S. and Olney, J. W.** (1989). Hypobaric-ischemic conditions produce glutamate-like cytopathology in infant rat brain. *J. Neurosci.* **9**, 1693-1700.
- Jackson, C. E. and Bryan, W. W.** (1998). Amyotrophic lateral sclerosis. *Semin. Neurol.* **18**, 27-39.
- Kakizuka, A.** (1998). Protein precipitation: a common etiology in neurodegenerative disorders? *Trends Genet.* **14**, 396-402.
- Lee, H. K., Kameyama, K., Huganir, R. L. and Bear, M. F.** (1998). NMDA induces long-term synaptic depression and dephosphorylation of the GluR1 subunit of AMPA receptors in hippocampus. *Neuron* **21**, 1151-1162.
- Linden, D. J., Smeyne, M. and Connor, J. A.** (1993). Induction of cerebellar long-term depression in culture requires postsynaptic action of sodium ions. *Neuron* **11**, 1093-1100.
- Lissin, D. V., Carroll, R. C., Nicoll, R. A., Malenka, R. C. and von Zastrow, M.** (1999). Rapid, activation-induced redistribution of ionotropic glutamate receptors in cultured hippocampal neurons. *J. Neurosci.* **19**, 1263-1272.
- Macklis, J. D. and Madison, R. D.** (1990). Progressive incorporation of propidium iodide in cultured mouse neurons correlates with declining electrophysiological status: a fluorescence scale of membrane integrity. *J. Neurosci. Methods* **31**, 43-46.
- Malenka, R. C. and Nicoll, R. A.** (1999). Long-term potentiation - a decade of progress? *Science* **285**, 1870-1874.
- Maletic-Savatic, M., Malinow, R. and Svoboda, K.** (1999). Rapid dendritic morphogenesis in CA1 hippocampal dendrites induced by synaptic activity. *Science* **283**, 1923-1927.
- Man, Y. H., Lin, J. W., Ju, W. H., Ahmadian, G., Liu, L., Becker, L. E., Sheng, M. and Wang, Y. T.** (2000). Regulation of AMPA receptor-mediated synaptic transmission by clathrin-dependent receptor internalization. *Neuron* **25**, 649-662.
- Matesic, D. F. and Lin, R. C.** (1994). Microtubule-associated protein 2 as an early indicator of ischemia-induced neurodegeneration in the gerbil forebrain. *J. Neurochem.* **63**, 1012-1020.
- McCarty, N. A. and O'Neil, R. G.** (1992). Calcium signaling in cell volume regulation. *Physiol. Rev.* **72**, 1037-1061.
- Midtgaard, J.** (1994). Processing of information from different sources: spatial synaptic integration in the dendrites of vertebrate CNS neurons. *Trends Neurosci.* **17**, 166-173.
- Nagy, Z.** (1999). Mechanisms of neuronal death in Down's syndrome. *J. Neural. Transm. Suppl.* **57**, 233-245.
- Nellgard, B. and Wieloch, T.** (1992). Postischemic blockade of AMPA but not NMDA receptors mitigates neuronal damage in the rat brain following transient severe cerebral ischemia. *J. Cereb. Blood Flow Metab.* **12**, 2-11.
- Olney, J. W.** (1971). Glutamate-induced neuronal necrosis in the infant mouse hypothalamus. An electron microscopic study. *J. Neuropathol. Exp. Neurol.* **30**, 75-90.
- Park, J. S., Bateman, M. C. and Goldberg, M. P.** (1996). Rapid alterations in dendrite morphology during sublethal hypoxia or glutamate receptor activation. *Neurobiol. Dis.* **3**, 215-227.
- Parker, J. C.** (1988). Volume-activated transport systems in dog red blood cells. *Comp. Biochem. Physiol. A* **90**, 539-542.
- Racca, C., Stephenson, F. A., Streit, P., Roberts, J. D. and Somogyi, P.** (2000). NMDA receptor content of synapses in stratum radiatum of the hippocampal CA1 area. *J. Neurosci.* **20**, 2512-2522.
- Ramón y Cajal, S.** (1909). Histologie du système nerveux de l'homme et des vertèbres. Paris: Maloine.
- Rose, C. R. and Konnerth, A.** (2001). NMDA receptor-mediated Na<sup>+</sup> signals in spines and dendrites. *J. Neurosci.* **21**, 4207-4214.
- Sarkadi, B., Attisano, L., Grinstein, S., Buchwald, M. and Rothstein, A.** (1984). Volume regulation of Chinese hamster ovary cells in anisoosmotic media. *Biochim. Biophys. Acta* **774**, 159-168.
- Shaw, P. J.** (1993). Excitatory amino acid receptors, excitotoxicity, and the human nervous system. *Curr. Opin. Neurol. Neurosurg.* **6**, 414-422.
- Sheardown, M. J., Nielsen, E. O., Hansen, A. J., Jacobsen, P. and Honore, T.** (1990). 2,3-Dihydroxy-6-nitro-7-sulfamoyl-benzo(F)quinoxaline: a neuroprotectant for cerebral ischemia. *Science* **247**, 571-574.
- Shoubridge, E. A.** (1998). Mitochondrial encephalomyopathies. *Curr. Opin. Neurol.* **11**, 491-496.
- Young, A. B.** (1997). Impairment of energy metabolism and excitotoxic cell death in Huntington disease. *Rev. Neurol. (Paris)* **153**, 496-498.
- Yu, X. M. and Salter, M. W.** (1998). Gain control of NMDA-receptor currents by intracellular sodium. *Nature* **396**, 469-474.